THE UV SPECTRUM OF THE BINARY SYSTEM TY PYX*

E. DANEZIS, E. ANTONOPOULOU, and E. THEODOSSIOU

Section of Astrophysics, Astronomy and Mechanics, Department of Physics, University of Athens, Zografos, Greece

(Received 10 April, 1992)

Abstract. A detailed list and analysis of line identifications of five UV spectra of the RS CVn-type binary system TY Pyxidis are presented. These spectra are recorded at different phases with the International Ultraviolet Explorer (IUE). Two of them are in the wavelength range $\lambda\lambda$1235–1950 Å while the other three in the range $\lambda\lambda$2700–3110 Å.

The far-UV spectrum of TY Pyx is mainly an emission spectrum dominated by the emission lines of the ions: C I, O I, C II, Si II, He II, Al II, and Fe III. We also pointed out the existence of a Fe III [34] line in absorption.

The UV spectrum between 2700–3110 Å is dominated by weak absorption lines. Two satellite components are indicated for many lines, which correspond to the two stars of the system, in the two out of the three spectra (LWP 13386 and LWP 13347).

Violet emission wings are observed for Fe I [1], Ti I [1], O IV [1], and Si III [1]. The UV spectrum of TY Pyx is also characterized by the multi-structure of Mg II [1] resonance lines.

1. Introduction

TY Pyx (≡ HD 77137 ≡ BV 811; ≡ BD − 276141; p = 3.198584 days) has been found to be an eclipsing system (Strohmeier, 1967). Popper (1969) has discovered that the H and K lines of Ca II in absorption and in emission are visible in the spectra of both components, thus he classified TY Pyx as an RS CVn-type system.

Photoelectric observations of TY Pyx in *ubvy* by Andersen *et al.* (1981) and in *JHK* by Antonopoulou (1983) clearly reveal that small wave-like distortion is present in the light curve, similar to that observed in the most of the RS CVn systems. No infrared excess has been observed from the system (Antonopoulou, 1983; Busso *et al.*, 1987).

Today it is known (Strassmeier *et al.*, 1988) that TY Pyx is an RS CVn-type binary system with two components of the same spectral type (G5IV), nearly equal masses (1.22 $M_\odot$ and 1.20 $M_\odot$, for the hot and the cool component, respectively) and also nearly equal radii (1.59 $R_\odot$ for the hot and 1.68 $R_\odot$ for the cool component).

The short wavelength ($\lambda\lambda$1235–1950 Å) low-resolution far UV spectra of TY Pyx have been given by Fernandez-Figueroa *et al.* (1985). These spectra present very well-defined emission features from low-ionization (e.g., O I) to high-ionization (e.g., N V) stages. Fernandez-Figueroa *et al.* (1985) have studied the low-resolution spectrum, SWP 19234, of TY Pyx and they have reported the presence of the well-defined lines: N V, O I, C II, Si IV, C IV, Si II, He II, C I, and Si III. Fernandez-Figueroa *et al.* (1986) studied the Mg II emission doublet at phase 0.54, for which they found a relative velocity

* Based on data from the International Ultraviolet Explorer, de-archived from the Villafranca Data Archive of the European Space Agency.

Astrophysics and Space Science **200**: 47–65, 1993.

of the components of TY Pyx of about 48 km s^{-1}. They also pointed out the existence of an absorption feature at the blue side of the Mg II line for which they suggest that it could be caused by local interstellar medium.

In this work we present an analysis of two far-UV spectra of TY Pyx ($\lambda\lambda$1235–1950 Å) and also of three other high-resolution spectra in the wavelength region $\lambda\lambda$2700–3110 Å which have been taken at different phases.

2. Observations

This work is based on five IUE spectra, which have been taken at different phases. Two of them are low resolution far UV spectra (SWP 11018 and SWP 19234) while the other three are high resolution UV spectra (LWR 9689, LWP 13347, and LWP 13386).

All the information connected with these spectra is given in Table I.

TABLE I

IUE images of TY Pyxidis

Image No.	UT times year–day–hours, min	Exposure times (min)	Phase	Names associated with the spectra
SWP 11018	1981–011–01:21	150	0.550	T. Simon, J. L. Linsky
SWP19234	1983–041–09:21	150	0.259	F. Figueroa, A. Gimenez, E. de Castro
LWR 9689	1981–011–00:20	40	0.537	T. Simon, J. L. Linsky
LWP 13347	1988–154–19:20	35	0.592	Bookbinder, J. Neff
LWP 13386	1988–160–05:54	30	0.295	J. Neff

The phases were calculated using the ephemeris given by Strassmeier *et al.* (1988).

The spectra were extracted from de-archived IUE images from the World Data Center (RAL) using the IUEDR package on STARLINK (Gidding, 1983).

Further analysis of the spectra was performed using the DIPSO package also available on STARLINK (Howarth and Murray, 1987).

The line identifications were performed on the basis of the multiplet tables of Moore (1968) and Kelly (1979).

The precision of the observed line position is limited by the IUE spectrum resolution (the low resolution is 5 Å and the high 0.2 Å) and by the blending due to the crowding of the lines.

3. Results and Discussion

3.1. The far-UV spectra (SWP 11018, SWP 19234)

The far-UV spectra of TY Pyx in the region 1235 Å to 1950 Å show emission profiles for the resonance lines of N V, C IV, Si IV. The N V resonance lines at 1240 Å are blended. The same happens for the C IV resonance doublet at 1550 Å.

Emission lines of C I [2], O I [2], C II [1], He II [2], Al II [2], and Fe III multiplets [51], [52], [62], [68], and Si II [1] probably blended with S I [2], have been found in the far-UV.

It is not possible the reliable estimation of the R.V., because of the low resolution (5 Å) of the available spectra.

The comparison of the far-UV spectra SWP 11018 and SWP 19234 of TY Pyx with the Kurucz's model, shows the existence of a deep and broad absorption line at about 1920 Å, which coincides with a blend of two very strong lines of Fe III [34] $\lambda\lambda$1914.056 and 1926.30 Å (Figure 1).

Figure 1 gives the low-resolution spectra of TY Pyx (SWP 11018, SWP 19234). The

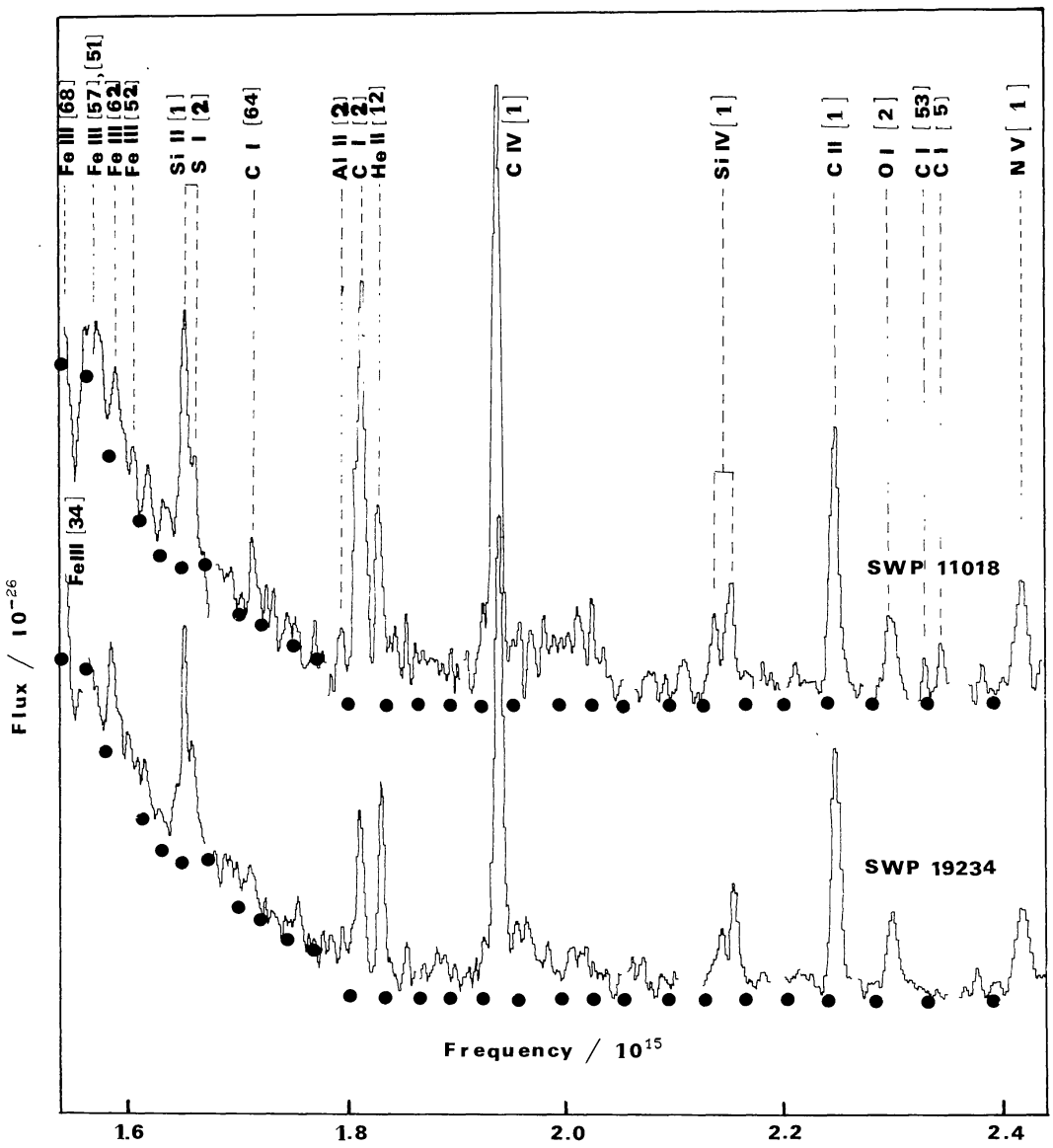

Fig. 1. The low-resolution spectra of TY Pyx, SWP 11018, and SWP 19234. The dots represent the points of the Kurucz (1979) photospheric model for T_{eff} = 5500 K and log g = 4.0.

dots represent the points of the Kurucz (1979) photospheric model for $T_{\rm eff}$ = 5500 K and $\log g$ = 4.0.

TABLE II

The observed emission lines of TY Pyx in the far UV

Ion	$\lambda_{\rm lab}$ (Å)	Mult.	Int.
N V	1238.821	1	1000
N V	1242.778	1	800
C I	1280.330	5	700
C I	1288.420	53	500
Si IV	1393.755	1	1000
Si IV	1402.770	1	800
C IV	1548.185	1	1000
C IV	1551.770	1	950
He II	1640.474	12	600
C I	1657.007	2	1000
Al II	1670.786	2	1000
C I	1751.820	64	800
Si II	1808.012	1	150
S I	1807.310	2	550
Si II	1816.927	1	200
S I	1820.342	2	500
S I	1826.245	2	450
Fe III	1869.828	52	650
Fe III	1871.150	52	600
Fe III	1882.047	62	650
Fe III	1882.972	62	250
Fe III	1883.816	62	200
Fe III	1884.596	62	550
Fe III	1918.284	57	450
Fe III	1922.789	51	1000
Fe III	1952.640	68	700
Fe III	1953.320	68	900
Fe III	1953.480	68	650

Table II gives the list of emission lines observed in the far UV spectra of TY Pyx (SWP 11018, SWP 19231). The successive columns in Table II give:

(1) The ion corresponding to the line.
(2) The laboratory wavelength in Å for each line.
(3) The multiplet number.
(4) The intensity of the line (Moore, 1968).

3.2. The UV spectra (LWR 9689, LWP 13347, and LWP 13386)

The UV spectra of TY Pyx LWR 9689, LWP 13347, and LWP 13386 ($\lambda\lambda$2700–3110 Å) are emission spectra; though, a weak absorption spectrum also co-exists in all the three given spectra. These spectra are mainly characterized by the Mg II [1] emission resonance doublet, which presents a multiple structure. This emission feature, in the

spectra LWR 9689 (p. 0.537) and LWP 13347 (p. 0.592), is also blended with strong absorption lines of Mg II [1]. Strong violet emission wings are present for a great number of ions at the phases 0.537 and 0.592 (LWR 9689, LWP 13347, respectively), but they have been disappeared at phase 0.295 (LWP 13386).

The most examined ions in the spectra LWP 13347 (p. 0.592) and LWP 13386 (p. 0.295), present two absorption components, which correspond to the two stars of the system. The mean radial velocities for the three phases are given in Table VI.

Table III gives the list of absorption lines observed in the spectra of TY Pyx (LWR 9689, LWP 13347, and LWP 13386) except the Mg II [1] resonance doublet and the ions which present a violet emission wing. The successive columns in Table III give:

(1) The ion corresponding to the absorption line.
(2) The laboratory wavelength in Å for each absorption line.
(3) The intensity of the line (Kelly, 1979).
(4) The multiplet number.

The next nine columns of Table III give the measured wavelength (λ mes), the difference $\Delta\lambda$ and the radial velocity (R.V.) for the three spectra, respectively.

The detection of an interstellar line was not possible because of the blends, so we could not measure a probable line shift.

Figures 2 to 7 show a collection of spectral region in the long wavelength spectra of TY Pyxidis.

3.2.1. *Violet emission wings*

One of the most remarkable feature in the long wavelength region of the IUE spectra of TY Pyx is the violet emission wings, which correspond to a great number of ions of a large ionization potential scale.

This phenomenon is an indication of mass exchange between the two stars of the system.

Violet emission which are detectable for the following spectra lines of the ions: Fe I multiplets [1] and [9], Ti I [1], Si III [1], and O IV [1] (Table IV).

Table IV gives a list of the lines which present this type profile.

The successive columns in Table IV give:

(1) The laboratory wavelength in Å for each line.
(2) The ion corresponding to the line.
(3) The multiplet number.
(4) The intensity of the line (Kelly, 1979).

The next 9 columns of Table IV gives the emission peak (e.p.), the absorption core (a.c.) and the red edge (r.e.) of the line respectively for the three given spectra.

Figures 2, 3, 6, and 7 show a collection of spectral regions in the long wavelength spectra of TY Pyx between $\lambda\lambda$2700–3110 Å, which present a violet emission wing.

3.2.2. *The Mg II [1] Resonance Doublet*

Another one remarkable feature in the long wavelength region of the IUE spectra of TY Pyx is the Mg II [1] emission resonance doublet which is characterized by a multiple structure.

TABLE III

The observed absorption lines of TY Pyx in UV

Ion	λ_{lab}	Int.	Mult.	λ_m (LWR 9689)	$\Delta\lambda$	u_1	λ_m (LWP 13386)	$\Delta\lambda$	u_2	λ_m (LWP 13347)	$\Delta\lambda$	u_3
Fe III	2702.65	40	–	2702.55	−0.10	−11.10	–	–	–	2702.65	0.00	0.00
Fe III	2704.42	25	159	2704.25	−0.17	−18.86	2703.80	−0.62	−68.78	–	–	–
Fe II	2714.414	80	63	2715.00	−0.586	64.76	–	–	–	2715.00	0.586	64.76
							2716.40	1.99	220.00	2716.00	1.586	175.28
Fe I	2719.027	620	5	2719.60	0.573	63.22	2719.30	0.273	30.12	2719.55	0.523	57.70
							2720.95	1.923	212.17	2720.65	1.623	179.07
Fe I	2720.902	380	5	2721.30	0.398	43.88	2720.95	0.05	5.51	2721.20	0.298	32.85
							2722.50	1.60	176.41	2722.30	1.398	154.14
Fe II	2724.879	9	62	–	–	–	–	–	–	2725.00	0.121	13.32
							–	–	–	2726.35	1.471	161.95
Fe II	2727.538	80	63	2728.20	0.662	72.81	2727.80	0.270	29.70	2727.85	0.312	34.31
							2729.80	2.262	248.80	2728.30	0.762	83.81
Fe II	2736.968	650	63	2737.20	0.232	25.43	2736.95	0.018	2.19	–	–	–
							2738.95	1.982	217.24	–	–	–
Fe II	2739.545	200	63	2739.80	0.255	27.92	2739.30	−0.245	−27.37	2739.40	−0.145	−15.87
							2741.20	1.655	181.23	2740.80	1.255	137.43
Fe II	2746.483	170	62	2746.65	0.163	17.80	2746.75	0.263	28.72	2747.05	0.563	61.49
blend							2747.90	1.413	154.34	2747.55	1.063	116.11
C II	2746.488	250	15									
Fe II	2746.978	870	63	2747.10	0.122	13.32	2747.15	0.172	18.78	2747.55	0.572	62.46
blend							–	–	–	–	–	–
C II	2747.31	350	15									
Fe II	2749.178	750	63				–	–	–	–	–	–
Fe II	2749.324	100	62	2749.50	0.180	19.64	2749.75	0.426	46.48	2749.85	0.526	57.40
							2751.05	1.726	188.33	2750.45	1.126	122.86
Fe II	2749.482	220	63	2749.75	0.265	28.91	2749.90	0.418	45.60	2750.00	0.518	56.52
							2751.35	1.868	203.82	2750.70	1.220	133.11
Fe I	2750.140	250	5	2750.55	0.410	44.72	2750.80	0.660	71.99	2750.70	0.560	61.08
							2752.10	1.960	213.80	2751.55	1.41	153.81
Fe II	2753.289	80	235	–	–	–	2753.20	−0.089	−9.80	–	–	–
							2755.10	1.811	197.32	–	–	–

Table III (continued)

Ion	λ_{lab}	Int.	Mult.	λ_m (LWR 9689)	$\Delta\lambda$	u_1	λ_m (LWP 13386)	$\Delta\lambda$	u_2	λ_m (LWP 13347)	$\Delta\lambda$	u_3
Fe II	2755.733	280	62	2756.00	0.267	29.06	2755.70	−0.03	−3.26	2755.80	−0.03	−3.26
							2757.20	1.47	160.00	2756.65	0.917	98.83
Ti I	2757.397	60	30	2757.75	–	–	2757.75	0.353	38.406	2758.20	0.803	87.36
							2759.50	2.103	228.80	2758.80	1.403	152.65
Fe II	2767.500	750	235	2767.55	0.05	5.42	2767.70	0.20	21.68	2768.00	0.50	54.20
blend							2768.50	1.00	108.40	–	–	–
Fe II	2767.500	750	373									
Mg I	2776.695	130	6	2777.50	0.76	82.37	2776.90	0.21	22.68	2777.25	0.55	59.42
							2778.75	2.055	222.00	2778.75	2.05	221.50
Mg I	2778.277	130	6	2778.65 ?	0.37	39.95	2778.40	0.123	13.28	2778.20	0.92	99.34
							2780.10	1.82	196.52	2779.80	1.52	164.13
Mg I	2779.832	160	2	–	–	–	2780.10	0.26	28.06	2780.40	0.57	61.51
							2781.60	1.77	191.00	2781.60	1.77	191.00
O V	2781.01	1000	–	2781.20	0.20	21.57	2781.20	0.19	20.50	2781.60	0.59	63.64
							2783.05	2.04	220.00	2782.95	1.94	209.30
Mg I	2781.418	130	6	2782.75	1.33	143.45	2781.60	0.18	19.41	2782.00	0.58	62.55
							2783.40	1.98	213.56	2783.40	1.98	213.56
Mg I	2782.974	130	6	2783.00	0.02	2.15	2783.05	0.07	7.54	2773.40	0.43	46.35
							2784.80	1.83	197.27	2784.70	1.73	186.50
O V	2789.85	775	–	2789.90	0.05	5.38	2790.25	0.40	43.01	2790.50	0.65	69.89
							–	–	–	–	–	–
Mg II	2790.768	150	3	2790.90	0.13	13.97	2790.90	0.13	14.02	2791.35	0.58	62.35
							–	–	–	–	–	–
C II	2836.710	1000	13	2837.00	0.29	30.67	–	–	–	2837.10	0.39	41.24
							–	–	–	2838.00	1.29	136.43
C II	2837.602	800	13	–	–	–	–	–	–	2837.85	0.248	26.22
										2838.75	1.148	121.37
Mg I	2852.120	1000	1	2852.40	0.28	29.45	2852.15	0.03	3.16	2852.05	−0.07	−7.36
							–	–	–	–	–	–
S III	2856.02	400	15	–	–	–	–	–	–	2856.20	0.18	18.91
										2857.15	1.13	118.70
Fe II	2858.340	550	279	2858.40	0.06	6.30	2858.340	0.00	0.00	2858.40	0.06	6.30
							2859.20	0.86	90.26	2859.15	0.81	85.01

Table III (continued)

Ion	λ_{lab}	Int.	Mult.	λ_m (LWR 9689)	$\Delta\lambda$	u_1	λ_m (LWP 13386)	$\Delta\lambda$	u_2	λ_m (LWP 13347)	$\Delta\lambda$	u_3
S III	2863.53	500	15	–	–	–	2862.80	– 0.73	– 76.48	–	–	–
							2864.20	0.67	70.19	2864.10	0.57	59.72
Fe II	2873.399	450	273	gap in spectrum								
Si I	2881.5792	1000	43	2881.90	0.3208	33.40	2881.60	0.02	2.08	2881.80	0.22	22.90
							2882.55	0.97	100.99	2882.40	0.82	85.37
O I	2883.780	100	30	2883.95	0.17	17.68	2883.90	0.12	12.48	2884.10	0.32	33.29
							–	–	–	–	–	–
S III	2904.310	300	15	2904.50	0.19	19.63	2904.35	0.04	4.13	2904.55	0.24	24.79
Si II	2904.283	300	17		0.217	22.42	–	–	–	–	–	–
Si II	2905.692	500	17	2906.40	0.708	73.10	2906.00	0.308	31.80	2905.80	0.108	11.15
				–	–	–	–	–	–	2907.15	1.458	150.53
Mg II	2928.625	80	2	2930.10	1.475	151.09	2929.60	0.975	99.88	–	–	–
							2931.30	2.675	274.02	–	–	–
Mg II	2936.496	100	2	2937.20	0.704	71.92	2936.50	0.004	0.41	–	–	–
							2938.25	1.754	179.19	2937.70	1.204	123.00
Ti I	2937.301	250	1	2938.25	0.949	96.92	2937.25	– 0.051	– 5.208	2937.70	0.399	40.75
							2939.40	2.099	214.38	–	–	–
Mg I	2938.473	60	3	2939.00	0.527	53.80	2938.25	– 0.223	– 22.77	2938.50	0.027	2.76
							–	–	–	–	–	–
Fe II	2939.506	110	60	2939.55	0.044	4.490						
Mn II	2939.312	550	5		0.238	24.29	2938.75	– 0.562	– 57.36	2939.70	0.388	39.60
Mg I	2941.990	70	3	2942.15	0.160	16.31	2942.15	0.160	16.31	–	–	–
							2944.15	2.16	220.26	–	–	–
Fe II	2944.399	12	78	gap in spectrum			2944.65	0.251	25.57	–	–	–
							–	–	–	–	–	–
Fe II	2947.658	750	78	2947.90	0.242	24.63	2947.70	0.042	4.27	–	–	–
Fe II	2949.178	450	277	2949.80	0.622	63.27	2949.50	0.322	32.75	2949.30	0.122	12.41
Mn II	2949.204	700	5	–	–	–	–	–	–	–	–	–
S III	2950.23	300	18	2950.50	0.27	27.46	2950.55	0.32	32.54	2950.20	10.03	– 3.05
							2915.25	0.02	2.03	2950.90	0.67	68.13
Fe II	2964.62	360	78	2965.80	1.18	119.41	–	–	–	–	–	–
Fe II	2970.510	15	60	2970.95	0.44	44.44	2970.51	0.00	0.00	2970.90	0.39	39.39
							2972.45	1.94	195.92	2972.70	2.19	221.17

Table III (continued)

Ion	λ_{lab}	Int.	Mult.	λ_m (LWR 9689)	$\Delta\lambda$	u_1	λ_m (LWP 13386)	$\Delta\lambda$	u_2	λ_m (LWP 13347)	$\Delta\lambda$	u_3
Fe II	2982.059	285	335	2982.25	0.191	19.21	2982.050	− 0.009	− 0.90	2982.70	0.641	64.48
							2983.95	1.891	190.24	2983.50	1.441	144.967
Fe I	2983.5698	320	9	2984.20	0.63	63.36	2983.50	− 0.070	− 21.05	2984.10	0.530	53.291
							2985.60	2.030	204.14	2985.10	1.530	153.863
Fe II	2984.831	50	78	2985.50	0.669	67.24	2985.10	0.269	27.04	2985.50	0.669	67.24
							2986.80	1.969	197.90	2986.50	1.669	167.75
Fe II	2985.545	750	78	2985.90	0.355	35.67	2985.50	− 0.045	− 4.52	2985.90	0.355	35.67
							2987.10	1.555	156.25	2987.00	1.455	146.20
Fe I	2999.5118	200	30	2999.600	0.0882	8.81	2999.30	− 0.2118	− 21.18	2999.20	−0.3118	− 31.18
							3000.80	1.2882	128.84	3000.40	0.8882	88.83
Fe II	3000.059	110	276	2999.950	0.109	10.90	–	− 1	–	2999.45	−0.609	− 60.899
							–	–	–	3001.10	1.041	104.098
Fe I	3000.977	280	9	3001.100	0.123	12.296	301.00	0.023	2.299	3000.95	−0.027	− 2.699
							3002.50	1.523	152.25	3002.20	1.223	122.26
Fe III	3001.617	650	9	3001.650	0.033	3.298	3001.40	− 0.217	− 21.688	3001.20	−0.417	− 41.68
							3002.90	1.283	128.231	3002.40	0.783	78.26
Fe II	3002.650	750	78	3003.20	0.55	54.95	3002.90	0.25	24.98	3003.00	0.35	34.97
							3003.90	1.25	124.89	3004.40	1.75	174.85
Fe I	3020.4907	220	9	–	–	–	3020.55	0.059	5.889	3020.60	0.1093	10.86
							3022.00	1.509	149.91	3022.00	1.5093	149.91
Fe I	3020.639	380	9	3020.70	0.061	6.058	–	–	–	–	–	–
							–	–	–	–	–	–
Fe I	3021.0727	240	9	3021.50	0.4273	42.43	3021.30	0.227	22.57	3021.50	0.4273	42.43
							3022.65	1.577	156.63	3023.10	2.0273	201.31
Fe I	3024.032	220	11	3024.30	0.268	26.59	–	–	–	–	–	–
							–	–	–	–	–	–
Fe I	3091.5769	110	28	3091.750	0.1731	16.797	3091.650	0.0731	7.093	–	–	–
							3093.20	1.6231	157.50	–	–	–

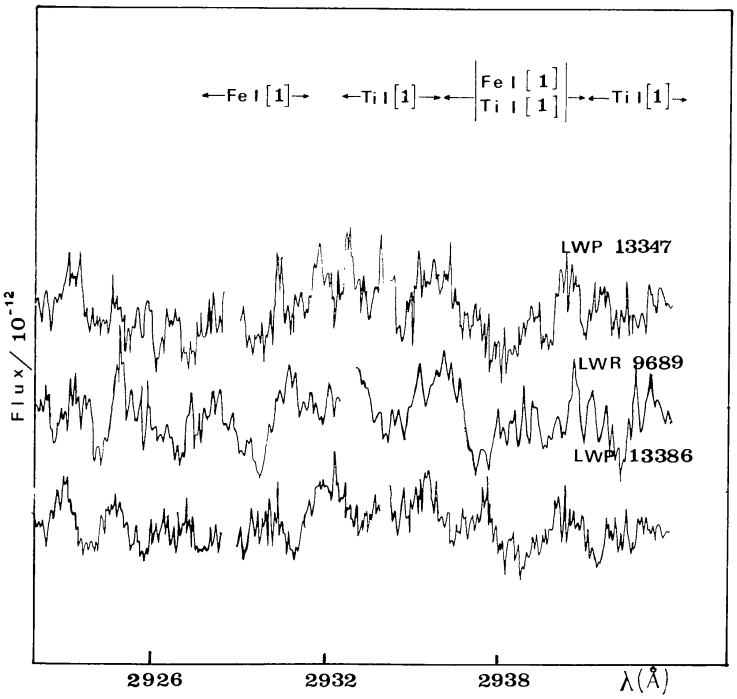

Fig. 2.

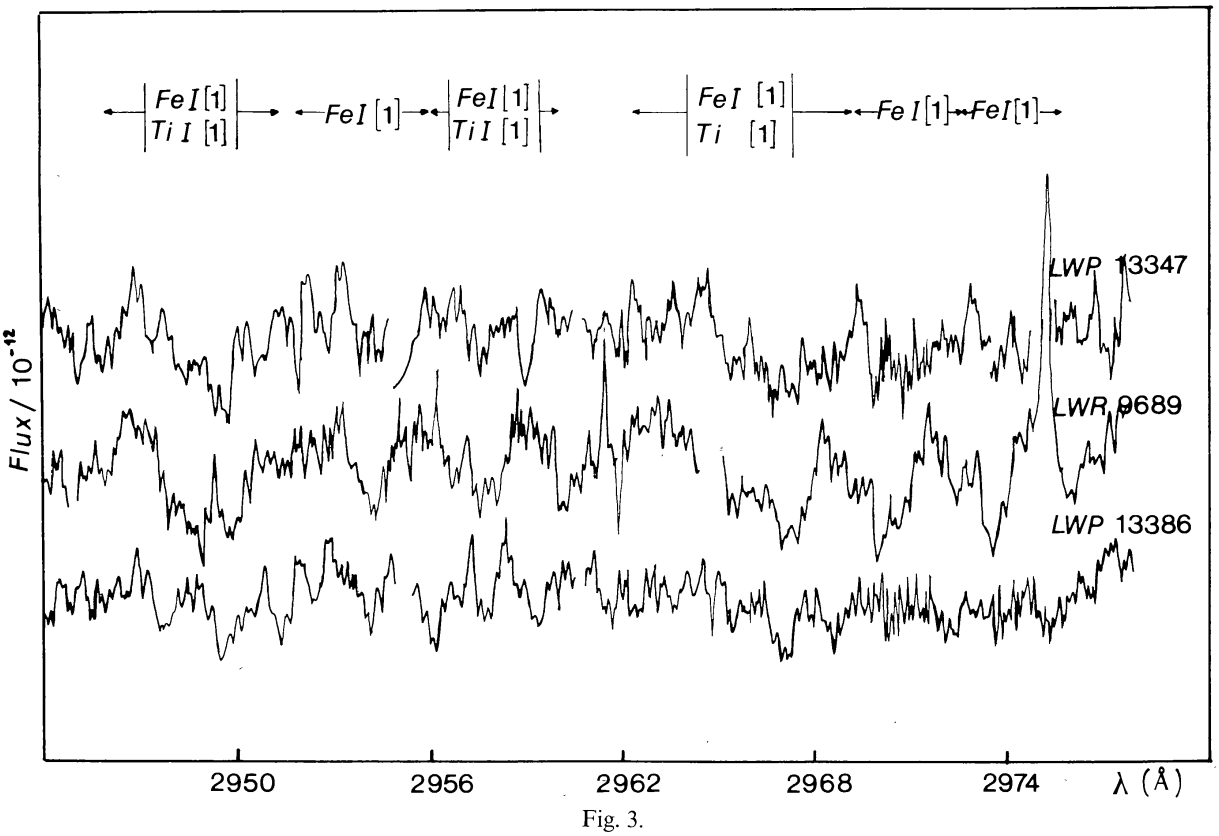

Fig. 3.

Fig. 2–7. Figures 2 to 7 show a collection of spectral region in the long wavelength spectra of TY Pyx. Figures 2, 3, 6, and 7 show a collection of spectral region in the long wavelength spectra of TY Pyx between $\lambda\lambda$2700–3110 Å, which present a violet emission wing.

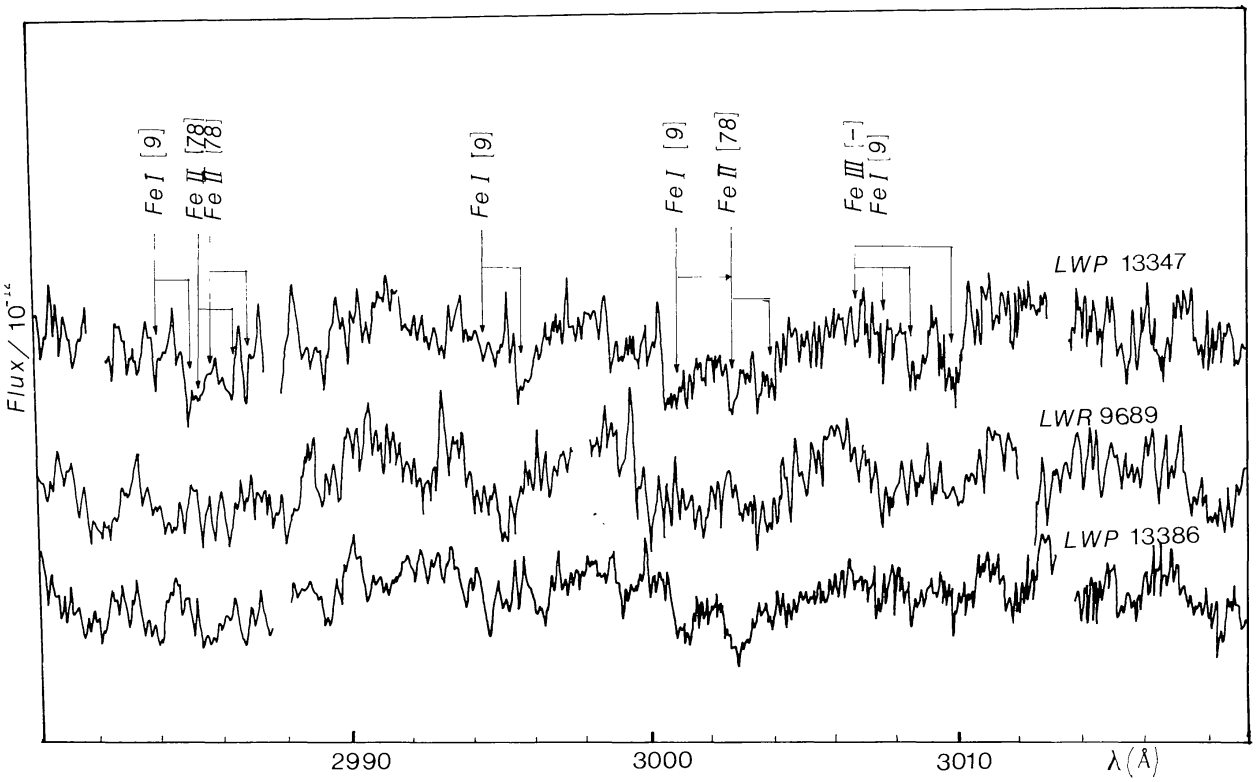

Fig. 4.

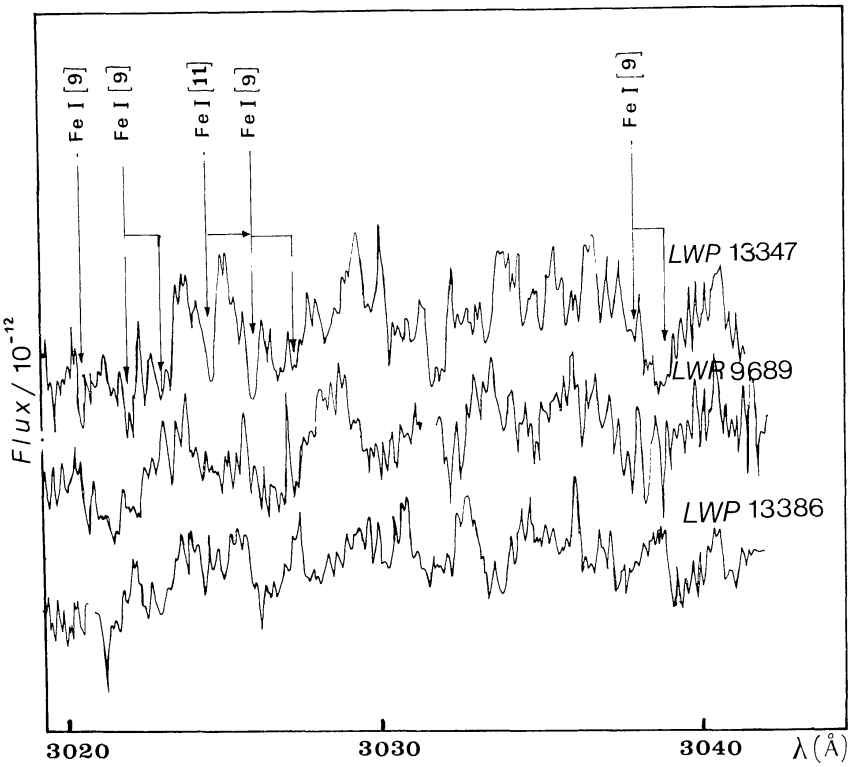

Fig. 5.

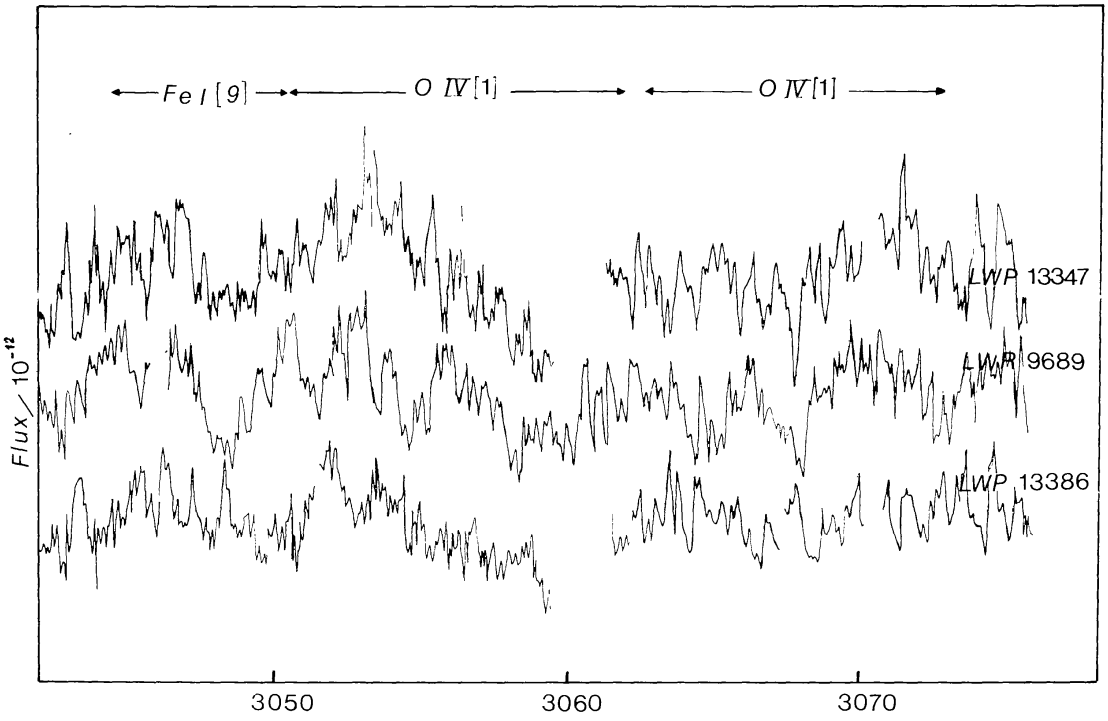

Fig. 6.

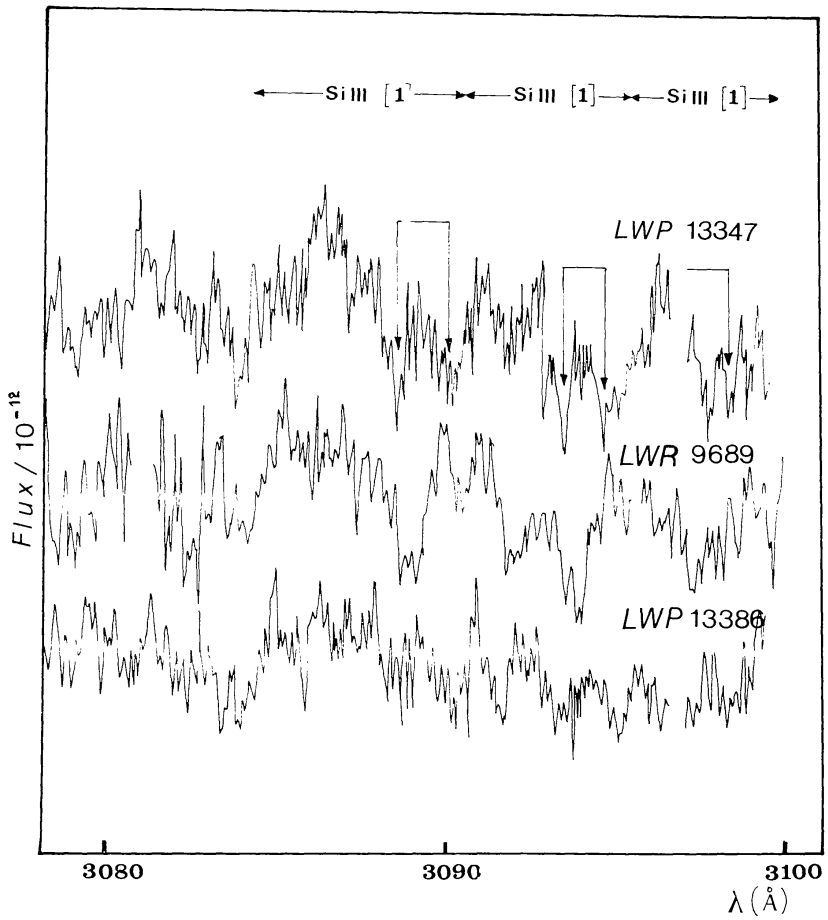

Fig. 7.

TABLE IV

Lines which present a violet emission wing

λ_{lab}	Ion	Mult.	Int.	LWR 9689			LWP 13386			LWP 13347		
				e.p.	a.c.	r.e.	e.p.	a.c.	r.e.	e.p.	a.c.	r.e.
2926.584	Fe II	60	10	2924.90	2927.00	–				–	–	–
2929.008	Fe I	1	110	2928.30	2929.70	–				–	–	–
2933.526	Ti I	1	250	–	2934.10	–				–	–	–
2936.9034	Fe I	1	340	2936.10	2937.20	2938.50				2935.60	2938.00	2939.30
2941.995	Ti I	1	600	2940.55	2942.150	2942.30				–	–	–
2947.877	Fe I	1	320	2946.70	2949.00	–				2946.90	2949.70	2950.30
2948.255	Ti I	1	600							–	2948.00	–
2953.940	Fe I	1	240	2953.40	2954.50	–				2953.40	–	–
2956.133	Ti I	1	700	2956.30	2957.750	–				–	2959.10	–
2956.796	Ti I	1	250									
2957.365	Fe I	1	155									
2966.8982	Fe I	1	380	–	2967.20	–				2964.80	2967.00	–
2967.220	Ti I	1	250							–		
2970.0995	Fe I	1	280	2968.50	2970.30	–				2969.40	2970.90	2972.20
2973.237	Fe I	1	220	2971.85	2973.85	–				–	–	–
2973.134	Fe I	1	340									
2994.4269	Fe I	9	320	2993.10	2995.20	2995.90				–	–	–
3008.139	Fe I	9	220	3006.30	3007.45	3009.00				–	–	–
3007.275	Fe III	–	650									
3025.8425	Fe I	9	220	3023.75	3026.40	–				3025.20	3026.00	3027.60
											3027.20	
3037.3887	Fe I	9	280	3036.00	3038.30	3039.30				3067.70	3038.70	–
3047.6043	Fe I	9	280	3046.20	3048.60	–				3046.80	–	–
3059.0856	Fe I	9	320	3056.00	–	–				–	–	–
3063.420	O IV	1	700	3053.20	–	–	3051.90	–	3063.50	3053.50	–	3061.50
3067.2441	Fe I	28	155	–	–	–						
3071.610	O IV	1	650	–	–	–				3070.65	–	–
3086.236	Si III	1	1000	3086.10	3086.10	–				3086.35	3090.10	–
											3088.50	
3093.424	Si III	1	640	3090.80	3093.90	–				3092.70	3094.60	–
				blend Fe I							3093.50	
3096.826	Si III	1	410	–	3097.35	3099.00				3096.20	3098.30	–
3096.890	Mg I	5	230	blend Mg I							3097.75	–

e.p. = emission peak; a.c. = absorption core; r.e. = red edge.

This resonance doublet is embedded in a blend of absorption lines of Mg II [1] (Table V).

Table V describes the spectrum of Mg II resonance doublet.

The successive columns in Table V give:

(1) The ion corresponding to the absorption line.

(2) The laboratory wavelength in Å for each absorption line.

(3) The intensity of the line (Kelly, 1979).

(4) The multiplet number.

The next nine columns of Table V give the measured wavelength (λ_{mes}), the difference $\Delta\lambda$ and the radial velocity of the three examined spectra, respectively.

The Mg II [1] resonance doublet present the following features in the three examined phases:

(a) *Phase 0.537 (LWR 9689):* a strong emission line is embedded in a blend of the two absorption lines of Mg II [1]. Weak satellites components are present (Figure 8).

(b) *Phase 0.592 (LWP 13347):* two strong emission lines are embedded in the above blend of Mg II [1]. Many satellite components are present.

(c) *Phase 0.295 (LWP 13386):* the above two emission lines are also present but the blend of the absorption lines does not exist.

Weak satellite components are present.

3.2.3. *Description of the Absorption UV Spectrum*

The majority of the spectral features observed in the IUE spectra of TY Pyx (LWR 9689, LWP 13347, LWP 13386) at $\lambda\lambda$2700–3110 Å wavelength region, is due to a thin absorption shell.

Below we present a summary of the more interesting atomic species with some brief comments on the possibility to be present or absent in the spectra of TY Pyx.

Carbon

It appears mainly as C II.

C II:the lines of this ion are present (multiplets 13, 15). Three lines of this ion $\lambda\lambda$2746.488 Å [15], 2747.31 Å [15], 2836.710 Å [13] are present.

One of the possible C II lines (λ2837.602 Å [13]) is not recorded in our spectra because of a gap in the vicinity.

Oxygen

O I: only one line of O I at λ2883.780 Å of low intensity is present.

O IV: two strong lines of multiplet [1] at $\lambda\lambda$3063.420 Å and 3071.610 Å are present.

O V: two strong unidentified lines at $\lambda\lambda$2781.01 Å and 2789.85 Å are present.

Magnesium

It appears as neutral and in the first ionization stage.

Mg I: seven lines of this ion: $\lambda\lambda$2776.695 Å [6], 2778.277 [6], 2779.832 [6], 2782.974 [6], 2852.120 [1], 2941.990 [3], and 3096.890 Å 230 [5] are present.

TABLE V

The Mg II resonance lines

Ion	λ_{lab}	Int.	Mult.	λ_m (LWR 9689)	$\Delta\lambda$	u_1	λ_m (LWP 13386)	$\Delta\lambda$	u_2	λ_m (LWP 13347)	$\Delta\lambda$	u_3
Mg II (E)	2795.52	400	1	2795.45 (E)	− 0.07	− 7.51	2795.60 (E)	0.08	8.58	2795.55 (E)	0.03	3.22
				–	–	–	2795.75 (E)	0.23	24.68	2795.80 (E)	0.28	30.05
				2795.85 (E)	0.33	35.41	2796.25 (E)	0.73	78.34	2796.20 (E)	0.62	66.54
				2796.00 (E)	0.48	51.51	2796.40 (E)	0.88	94.44	2796.35 (E)	0.83	89.07
				2796.20 (E)	0.68	72.97	2797.15 (E)	1.63	174.92	2796.80 (E)	1.28	137.36
				2796.40 (E)	0.88	94.43	2797.25 (E)	1.73	185.65	2797.05 (E)	1.53	164.19
				2796.90 (E)	1.38	148.09	2797.75 (E)	2.23	239.31	2797.50 (E)	1.98	212.48
Mg II (E)	2802.697	300	1	2802.55 (E)	− 0.147	− 15.73	2802.65 (E)	− 0.047	− 5.03	2802.85 (E)	0.153	16.38
				2803.05 (E)	0.353	37.78	2802.90 (E)	0.203	21.73	2803.00 (E)	–	–
				2803.20 (E)	0.503	53.84	2803.30 (E)	0.603	64.54	–	–	–
				–	–	–	2803.50 (E)	0.803	85.95	2803.50 (E)	0.803	85.95
				2803.40 (E)	0.703	75.24	2804.20 (E)	1.503	160.88	2803.95 (E)	1.253	134.12
				2803.55 (E)	0.853	91.31	2804.30 (E)	1.603	171.58	2804.30 (E)	1.603	171.58
				2803.75 (E)	1.053	112.71	2804.60 (E)	1.903	203.70	–	–	–
				2804.00 (E)	1.303	139.47	2804.80 (E)	2.103	225.11	–	–	–

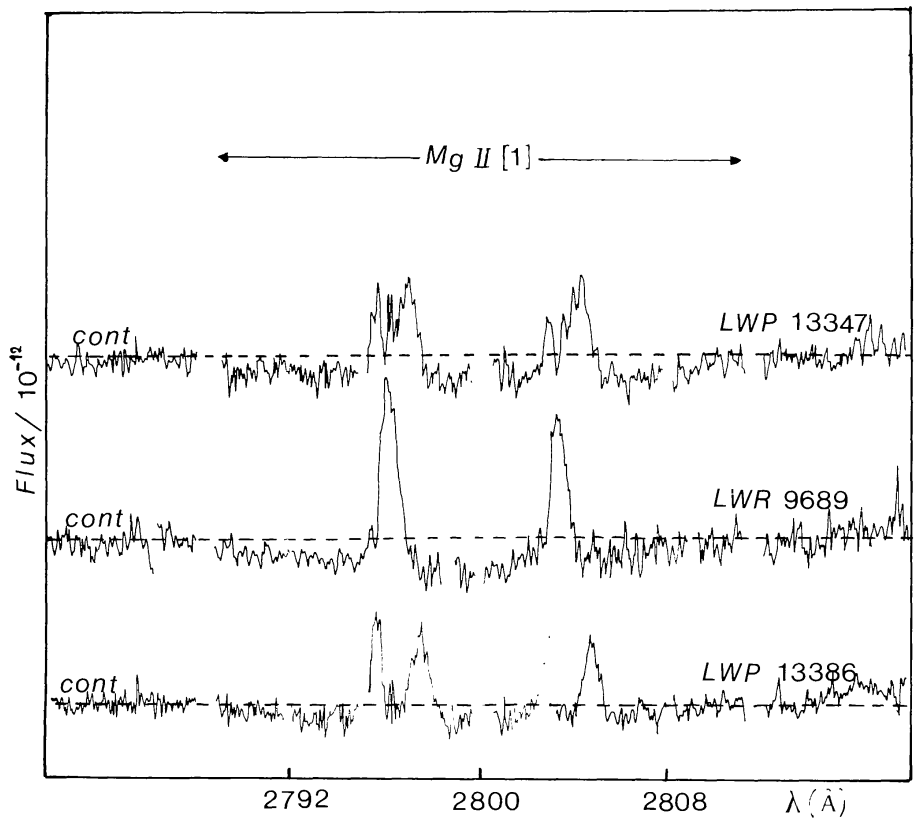

Fig. 8. Figure 8 gives the Mg II [1] resonance doublet, which is characterized by a multiple structure.

Mg II: the resonance lines of Mg II at $\lambda\lambda$2795.52 Å and 2802.697 Å are present (Section 3.2.2).

Apart from the two resonance lines of Mg II which are present, we also reported two lines of Mg II multiplet [3] at $\lambda\lambda$2790.768 Å and 2797.984 Å and another one of multiplet [2] at 2936.496 Å.

Silicon

This ion appears as neutral and in the first two ionization stages.

Si I: evidence is found for only one line of multiplet [13] at λ2881.597 Å.

Si II: two lines of this ion at $\lambda\lambda$2904.283 Å [17], 2905.692 Å are present.

Si III: two strong lines of multiplet [1] at $\lambda\lambda$3086.236 Å and 3093.424 Å are present.

Sulfur

S II: the presence of S II is uncertain blended with Mn II.

S III: this ion is possibly present. Four lines of S III at $\lambda\lambda$2856.02 Å 400 [15], 2863.53 500 [15], 2904.310 300 [15], and 2950.23 Å 300 [18] are present.

Titanium

Ti I: this ion is present. Only one line of Ti I was found at 2557.397 Å of multiplet [30]; but longward of 2930 Å the spectrum of Ti I multiplet [1] is evident: seven lines of multiplet [1] at λλ2933.526 Å, 2937.301, 2941.995, 2948.255, 2956.133, 2956.796, and 2967.220 Å are present.

Manganese

Mn II: two lines of Mn II of multiplet [5] at λλ2939.312 Å and 2949.204 Å are present.

Iron

Iron is the main contributor to the UV spectrum of TY Pyx. It appears as neutral and in the first two ionization stages.

Fe I: this ion is present (multiplets 5, 1, 9, 30, and 28).

Fe II: this ion is present (multiplets 62, 53, 235, 279, 273, 61, 60, 277, 373, 78, 335, and 276).

Fe III: two lines of low intensity were found. The line at λ2704.42 Å 25 [159] and the unclassified one at λ2702.65 Å. Longward of 3000 Å two strong lines were found at λλ3001.617 Å 650 [19] and 3007.275 Å 650 (unclassified). The strong line of Fe III at

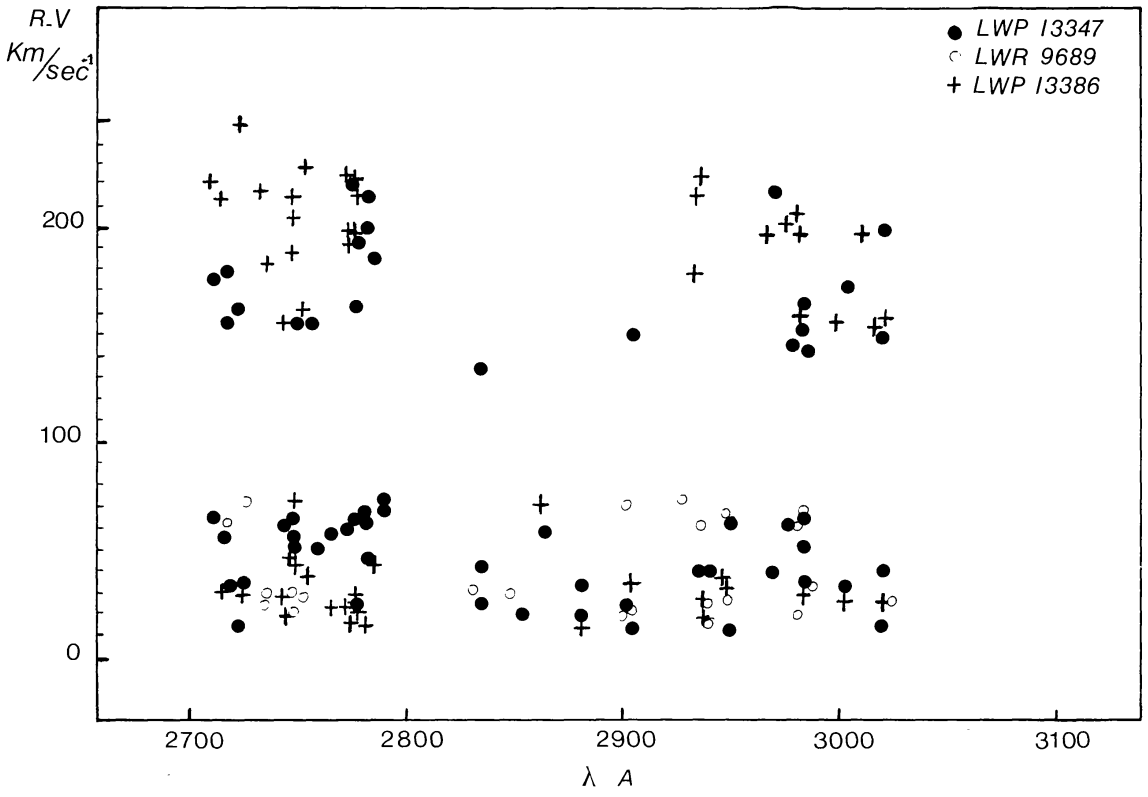

Fig. 9. Figure 9 gives the radial velocities of the noticeable absorption lines for the three spectra versus the wavelength.

TABLE VI

The mean radial velocities for the two components of the system

Image No.	UT times year–day–hours, min	Phase	R.V.	
			1st star	2nd star
LWR 9689	1981–011–00:20	0.537	47 ± 28	–
LWP 13347	1988–1594–19:20	0.592	56 ± 18	170 ± 33
LWP 13386	1988–160–05:54	0.295	32 ± 12	192 ± 33

λ3013.167 Å [9] is not recorded in our spectra because of a gap in the vicinity. There is no evidence of elements heavier than iron.

In Table VI we summarize the values of the radial velocities of the two components of the system. The successive columns give:

(1) The image number.

(2) UT times (year–day–hours, min).

(3) Orbital phase of the system.

(4) Radial velocities of the two components.

Figure 9 gives the radial velocities of the noticeable absorption lines for the three spectra versus the wavelength.

4. Conclusions

From the present work, using the five existing spectra of TY Pyx, we conclude to the following points:

(1) The far-UV spectrum ($\lambda\lambda$1235–1950 Å) of TY Pyx is mainly an emission spectrum. The emission lines we pointed out are: N V [1], Si IV [1], C IV [1], He II [12], C I [2], Al II [2], Si II [1], S I [2].

Apart of them we also detected in this paper the following absorption and emission lines:

(a) Emission lines of Fe III [51], [52], [62], [68] are detected in the spectral region $\lambda\lambda$1710–1950 Å.

(b) The comparison of the far-UV spectra SWP 11018 and SWP 19234 with the Kurucz's model, shows the existence of a weak, absorption shell. A deep broad absorption line at about 1920 Å, which coincides with a blend of two very strong lines of Fe III [34] $\lambda\lambda$1914.056 and 1926.30 Å is present (Figure 1).

(2) From the three UV spectra ($\lambda\lambda$2700–3110 Å), we pointed out:

(a) The existence of a weak absorption spectrum. For the phases 0.592 (LWP 13347) and 0.295 (LWP 13386), two absorption components have been detected for many absorption lines, which correspond to the two stars of the system.

(b) Violet emission wings are present for the lines Fe I [1] and [9], Ti I [1], Si III [1], and O IV [1] (Section 3.2.1).

(c) The Mg II [1] resonance doublet is characterized by a variable multiple emission

structure related to the phase, embedded in a blend of absorption lines of Mg II [1] (Section 3.2.2).

The binary system TY Pyx exhibits very interesting variations and we conclude with our hope that better quality UV images could be taken systematically to explain further the behaviour of this interesting system.

Acknowledgements

We would like to thank Mr M. Mathioudakis at the Armagh Observatory for his help in recovering the data from the database. Part of this work was done during the visit of one of us (E.A.) at the Armagh Observatory who thanks all the staff of the observatory for their hospitality.

References

Antonopoulou, E.: 1983, *Astron. Astrophys.* **120**, 85.
Andersen, J., Clausen, J. V., Nordstrom, B., and Reipurth, B.: 1981, *Astron. Astrophys.* **101**, 7.
Busso, M., Scaltriti, F., Persi, P., Robberto, M., and Silvestro, G.: 1987, *Astron. Astrophys.* **183**, 83.
Fernandez-Figueroa, M. J., de Castro, E., and Gimenez, A.: 1985, *Astron. Astrophys. Suppl.* **60**, 5.
Fernandez-Figueroa, M. J., Sedano, J. L., and de Castro, E.: 1986, *Astron. Astrophys.* **169**, 237.
Gidding, J. R.: 1983, *'IUEDR' STARLINK User*, Note 37, RAL.
Howarth, I. D. and Murray, M. J.: 1987, *'DIPSO' STARLINK User*, Note 50, RAL.
Kelly, R. L.: 1979, *Atomic Emission Lines in the Near Ultraviolet*, NASA, TM 80268
Kurucz, R. L.: 1979, *Astrophys. J. Suppl.* **40**, 1.
Moore, C. E.: 1968, *NBS Circ.*, No. 488.
Popper, D. M.: 1969, *Bull. Am. Astron. Soc.* **1**, 257.
Strassmeier, K. G., Hall, D. S., Zeilik, M., Nelson, E., Eker, Z., and Fekel, M. C.: 1988, *Astron. Astrophys. Suppl. Ser.* **72**, 291.
Strohmeier, W. 967, *Inf. Bull. Var. Stars*, No. 217.